Ordering and Roughening during the Epitaxial Growth of Alloys

J. R. Smith, Jr. and A. Zangwill
School of Physics, Georgia Institute of Technology, Atlanta, Georgia 30332
(Received 21 August 1995)

A kinetic mean field is used to study the interplay between compositional ordering and surface roughening during the epitaxial growth of a model lattice-matched binary alloy. Assuming that order is favored thermodynamically at the free surface only, the evolution of long range order and short range order is shown to depend nontrivially on the morphology of the film as determined by deposition conditions and the presence of energy barriers to atomic migration at surface step edges. A spatial interpretation of the results is offered that accords well with existing experimental data.

PACS numbers: 64.60.Cn, 68.55.–a, 81.10.Aj

Growth-induced surface roughening and growth-induced alloy ordering separately have attracted considerable attention from the community of physicists fascinated by epitaxial processes. Growth-induced ordering refers to the fact that epitaxial semiconductor alloys often exhibit long range order despite the fact that the corresponding bulk alloys favor phase separation. Growth-induced roughening refers to the morphological deviations from a flat surface profile that occur inevitably during epitaxial growth. Both effects are known to depend sensitively on growth conditions and substrate orientation. But, to our knowledge, only two recent experiments [1,2] and no theory have been addressed explicitly to the interplay between roughening processes and long range ordering processes.

A decade of intense study has been devoted to the problem of manipulating the degree of order in epitaxial semiconductor alloys. Experiment and theory have focused on the Si_xGe_{1-x} system [3] and especially the group III-V ternary alloys [4]. The observed ordering is known to be thermodynamically unstable in the bulk. But calculations show that ordering can be favored by local surface energetics, e.g., reconstructions of the flat surfaces or step edges. The consensus is that order is established in the near surface region and then "frozen-in" as growth proceeds. Interestingly, the same thermodynamic scenario has been predicted [5] for $Ni_3Pt(001)$ although, to our knowledge, no epitaxial growth experiments have been attempted for this system.

The past decade has also been witness to a sustained effort devoted to identifying the causes and consequences of surface roughening during epitaxial growth. Stochastic models have been popular lately [6], but mean field theories [7] are quite adequate to describe the most commonly observed types of surface roughening: step bunching [8] and three-dimensional (3D) island formation associated with either misfit strain relief [9] or the presence of relatively high energy barriers to interlayer atomic migration at step edges [10]. In the two alloy ordering experiments noted earlier, roughening due to the strain relief [1] and step bunching [2] mechanisms individually were operative. In the present work, we focus on roughening associated with step edge barriers, and thus restrict ourselves to the growth of lattice-matched alloys on nominally flat substrates.

Our analysis generalizes a kinetic mean field theory of the antiferromagnetic spin-one Ising model presented some years ago by Saito and Müller-Krumbhaar [11]. These authors examined the propagation of long range order (LRO) for a solid crystallizing from the vapor phase. Surface diffusion was not considered and the propagation of short range order (SRO) was not addressed. A subsequent variation of this theory examined SRO induced by surface diffusion but entirely neglected the possibility of LRO [12]. Most recently, Monte Carlo simulations of alloy growth have appeared that include step-exchange processes to induce order [13]. Unfortunately, the simulation algorithm used excluded the possibility of multilayer surface roughness.

The model system studied here is a simple cubic *AB* alloy growing in the (001) direction with nearest neighbor interactions ϵ_{AA}, ϵ_{BB}, and ϵ_{AB} chosen to favor rocksalt-type order. No change in the qualitative features we report is expected for crystal lattices that support more complex ordered structures so long as the constituent sublattices are interpenetrating. During growth, overhang structures are forbidden so that no bulk vacancies can occur. Bulk diffusion is thereby arrested, and the aforementioned phenomenon of kinetic freezing arises in a natural way. If we assign an integer label j to each crystal plane of N sites that grows parallel to the substrate, a Bragg-Williams theory [11] would suffice for the present purposes if the coverage in each layer $\theta(j)$ and LRO in each layer $\eta(j)$ were adequate to describe the surface morphology and state of order of the growing crystal. But, as will become apparent, a quantitative measure of the SRO in each layer $\sigma(j)$ and the step edge density in each layer $s(j)$ is essential for a correct description of the problem. For this reason, we adopt a layer-resolved, kinetic Bethe-Peierls approximation [14].

The details of this approximation have been discussed thoroughly in the literature [15]. Briefly, $\theta(j)$ is the

number density of atoms in layer j, $\eta(j)$ is the difference in the number densities of A atoms on the two sublattices of layer j, and $\sigma(j)$ and $s(j)$ are the number densities of AB and atom-vacancy nearest neighbor pairs in layer j. Internal consistency of the theory mandates that these four observables be supplemented by eight other related densities (whose physical meaning is less transparent) for each incomplete layer. A state vector $\mathbf{X}(t)$ is then defined so that the statistical averages of these variables constitute the components of the vector $\mathbf{x}(t) = \mathbf{X}(t)/N$. The time evolution of each component $x_k(t)$ obeys

$$\frac{d}{dt}\, x_k(t) = \sum_{\mathbf{\Delta}} \Delta_k \sum_{\mathbf{p}\in\mathbf{\Delta}} n[\mathbf{p}|\mathbf{x}(t)]\nu(\mathbf{p})e^{-E(\mathbf{p})/k_BT}, \quad (1)$$

where $\mathbf{\Delta}$ is a vector of integers that specifies the change $\mathbf{X} \rightarrow \mathbf{X} + \mathbf{\Delta}$ in the state of the system associated with each allowed Arrhenius-type kinetic process. The combinatoric factor $n[\mathbf{p}|\mathbf{x}(t)]$ is the Bethe-Peierls estimate of the number density of sites with local arrangements of the atomic species $\mathbf{p}$ compatible with $\mathbf{\Delta}$ given that the system average is fixed at $\mathbf{x}(t)$. The sum over $\mathbf{p}$ indicates that several local atomic arrangements are generally consistent with a given value of $\mathbf{\Delta}$ [16].

For a deposition event, the energy barrier $E(\mathbf{p}) = 0$, $\nu(\mathbf{p})$ is the mean arrival rate of atoms to the surface, and the two components of $\mathbf{p}$ respectively label the number of A atoms and B atoms in the first coordination shell around the site onto which deposition occurs. For a surface diffusion event, $\mathbf{p}$ is a four-component vector since the coordination shells of both the initial and final sites of the diffusing atom are involved, $\nu(\mathbf{p})$ is an attempt frequency, and we follow Ref. [14] and recent Monte Carlo simulations of epitaxial growth [17] by using the *initial* state energy of the local configuration as a bond-breaking estimate of the diffusion barrier $E(\mathbf{p})$. In particular, each nearest neighbor of an atom about to execute a surface diffusion jump makes a contribution of $|\epsilon_{AA}|$, $|\epsilon_{BB}|$, or $|\epsilon_{AB}|$ to the energy barrier so that both site coordination and chemical effects are included.

This paper reports results for an equiatomic alloy. The common deposition rate for A and B atoms is denoted F. For simplicity only, we choose $\epsilon_{AA} = \epsilon_{BB}$ and a single attempt frequency so that the *intralayer* surface diffusion rate for an isolated A atom bonded to an A atom immediately below itself is identical to the corresponding quantity for an isolated B atom bonded to a B atom immediately below itself. Their common diffusion constant is denoted D. We consider two morphological scenarios: (i) quasi-layer-by-layer growth obtained by equating the rates of interlayer and intralayer diffusion for a given initial state, and (ii) step-barrier-induced 3D growth obtained by setting the relevant *interlayer* diffusion attempt frequencies to zero. In all cases, the initial condition is a flat substrate with a specified degree of LRO. Gear's method [18] for stiff differential equations is used to propagate the nonlinear system defined by (1) forward in time.

We begin with the quasilayer growth scenario [7], where the computed time evolution of the total step density $s = \sum_j s(j)$, i.e., the surface roughness, exhibits undamped monolayer period oscillations with minima and maxima that decrease as D/F increases. Figure 1 shows the corresponding frozen-in, layer-averaged LRO and SRO for the case of deposition onto a perfectly ordered alloy substrate. The initial order cannot be maintained unless D/F is very large. Instead, the amount of LRO and SRO in each layer decreases as growth proceeds until a finite asymptotic value is reached. The latter is fixed by the deposition conditions (D/F) and the bond energy parameters, since it reflects the amount of order that can be established by surface diffusion and detachment and attachment processes in the time needed to deposit one monolayer. Note that the LRO approaches zero for the smallest D/F shown while the accompanying SRO approaches a nonzero constant. We interpret this result as the mean-field signature that antiphase boundaries (APB) are present in layer j since the SRO has been normalized so that a nonzero value indicates an excess of AB and BA nearest neighbor pairs compared to AA and BB pairs.

The trend seen in Fig. 1 can be understood as follows. A deposited atom either diffuses to a step or encounters another deposited atom. In either case, the occupied site may not be favored energetically, i.e., propagate order. If D/F is large enough, the atom has sufficient time to sample other sites and seek an energy minimum before it is frozen by the arrival of another atom onto itself. The substrate acts as a template so that all islands in

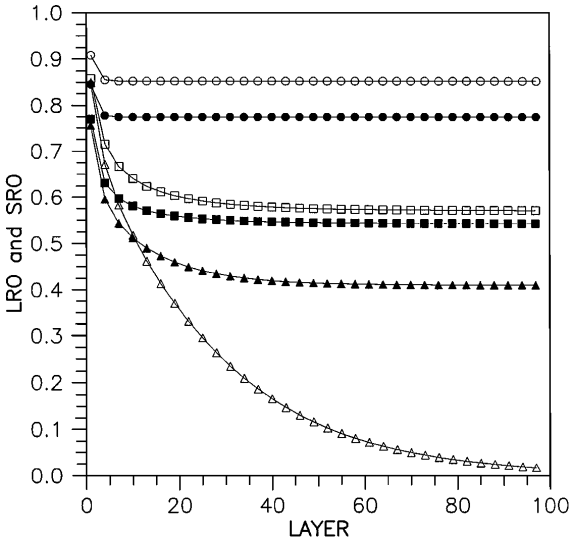

FIG. 1. The frozen-in LRO (open symbols) and SRO (filled symbols) in the first 100 layers of quasi-layer-by-layer growth for $D/F = 1.0 \times 10^5$ (△), 1.1×10^5 (□), and 2.0×10^5 (○). The substrate is fully ordered. The material parameters are $\epsilon_{AB} = -0.5$ eV, $\epsilon_{AA} = \epsilon_{BB} = -0.3$ eV, and $kT = 0.09$.

a layer (and subsequent layers) order in the same way. But as D/F decreases, the step density increases with a concomitant increase in the number of "mistakes" (an *AA* or *BB* pair) that form. Since the time available for the system to rearrange itself also decreases as D/F decreases, the number density of mistakes that freeze to yield APB's is inversely related to the normalized SRO. A zero value for LRO indicates that APB's separate domain variants of equal population.

We turn now to the case of infinite barriers to interlayer mass transport [7]. This situation where deposited atoms are confined to the terraces upon which they land is well understood to yield Poisson roughness associated with the formation of 3D "wedding-cake" structures [6,10]. This is reflected in our calculations by a monotonic increase in the total step density as deposition proceeds for all values of D/F. Figure 2(a) shows the corresponding frozen-in, layer-averaged LRO and SRO for the case of deposition onto a perfectly ordered alloy substrate. Both long and short range order decrease slowly at first until, without warning, the LRO drops to zero and the SRO drops to a nonzero value. The latter does *not* approach a constant asymptotic value as before but instead declines toward zero for as long as we followed its evolution. Larger values of D/F do not change this scenario; the drop occurs at larger film thickness, and the amount of residual SRO increases.

The initial slow decrease in LRO and SRO in Fig. 2(a) corresponds to the buildup of APB density as before. But the ever increasing surface roughness in this case results in an ever decreasing mean terrace length within the uppermost incomplete layers. The mean adatom migration distance decreases concomitantly so that the site sampling and compositional rearrangement processes needed to maintain long range order become less and less correlated within a given layer. The LRO collapses when the maximum roughness within these layers reaches a (D/F-dependent) critical value beyond which the repair of nascent APB's by surface diffusion becomes impossible. The template effect noted above guarantees that the onset of this phenomenon in a single layer is sufficient to propagate the effect to all higher layers. Calculations with a finite step edge barrier reveal that the abruptness of the loss of order lessens when the barrier height decreases.

An interesting feedback between the state of compositional order and the evolving crystal morphology is shown in Fig. 2(b). We plot here the value of the step density in each layer at the moment when it achieves its *maximum* value. Unlike the total step density, the monotonic increase of this quantity stalls immediately after the loss of LRO if D/F is large enough [cf. Fig. 2(a)]. Disordering evidently induces the system to smoothen. To gain insight into this curious phenomenon, we calculated the evolution of roughness and order beginning with a completely *disordered* substrate for $D/F = 5 \times 10^5$ (filled symbols). LRO never develops in this situation, and the maximum

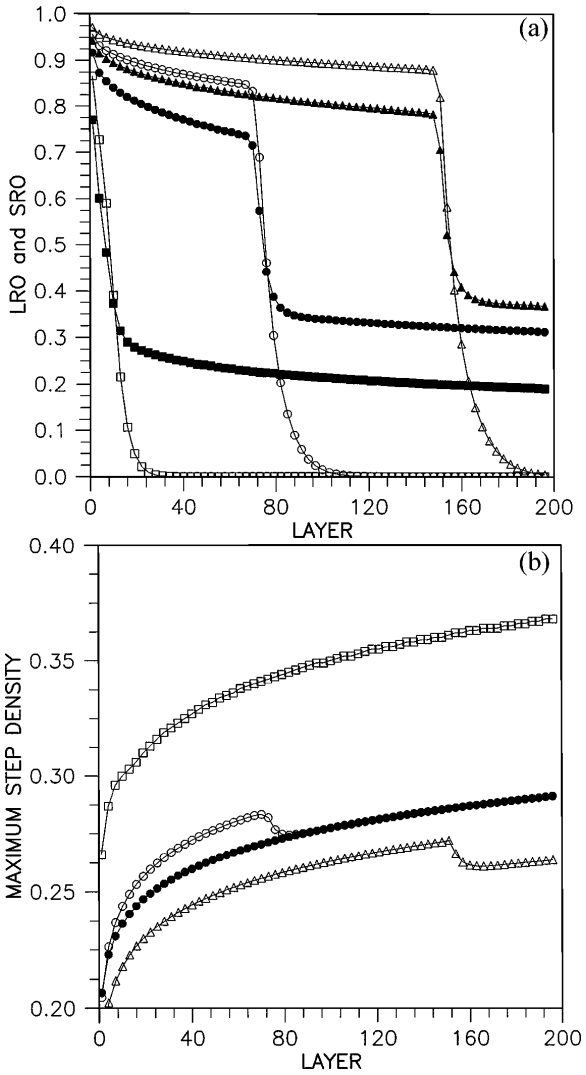

FIG. 2. (a) The frozen-in LRO (open) and SRO (filled) in the first 200 layers of step-barrier-induced 3D growth for $D/F = 1.0 \times 10^5$ (□), 5.0×10^5 (○), and 1.0×10^6 (△) on an ordered substrate. (b) The maximum step density in a layer under the same growth conditions as in (a) and $D/F = 5.0 \times 10^5$ (●) on a disordered substrate. The material parameters are the same as in Fig. 1.

roughness is *smaller* for the disordered system until the originally ordered material loses order. The coincidence of the two curves beyond that point demonstrates that, for fixed deposition conditions, a unique state of roughness is associated with the compositionally disordered state *independent* of the previous history of the sample.

A simple bond-breaking calculation shows that atom detachment from a step edge occurs more slowly when the layer immediately below is disordered rather than ordered. This shows up as smoothening in Fig. 2(b), since single adatoms contribute substantially to the state of maximum step density. For a finite step barrier, this argument can be replaced by an equivalent macroscopic argument that recalls that order prevails at the free surface in equilibrium. Any kinetically induced state of disorder

therefore possesses a higher surface free energy (surface tension) which then smoothens relatively more rapidly by capillarity. Both pictures are consistent with our observation that the magnitude of the roughness drop associated with the loss of order increases as D/F increases.

The most direct test of our predictions would be an "archaeology" experiment that reveals the degree of order in a film as a function of depth from the free surface. Unfortunately, the only experiment of this kind of which we are aware was performed for a film of GaInP grown under conditions where significant bulk diffusion occurred, thus obscuring the effects we find [19]. We encourage similar experiments for films grown with lower values of D/F. Otherwise, our results are in qualitative accord with existing experimental studies that correlate surface morphology with compositional ordering. The notion that a minimum average terrace width is required to support ordered regions is explicit in the discussion of Jesson *et al.* [1] of their *Z*-contrast electron microscopy results for a strain-roughened SiGe alloy grown on Si(001). Similarly, the atomic force microscopy results reported by Stringfellow *et al.* [2] include a strong correlation between the separation between step bunches on the surface of a GaInP alloy grown onto vicinal GaAs(001) substrates and the separation between APB's in the film as determined by transmission electron microscopy. It puzzled these authors that the APB density actually exceeded the bunch density for the smallest misorientations studied. This is not surprising in the present view since wedding-cake-type roughness may be expected in the large regions between bunches.

The authors acknowledge helpful discussions with Jerry Tersoff, Dimitri Vvedensky, David Jesson, and Jerry Stringfellow. This work was supported by the U.S. Department of Energy under Grant. No. DE-FG05-88ER45369.

[1] D. E. Jesson, S. J. Pennycook, J. Z. Tischler, J. D. Budai, J.-M. Baribeau, and D. C. Houghton, Phys. Rev. Lett. **70**, 2293 (1993).

[2] G. B. Stringfellow, L. C. Su, Y. E. Strausser, and J. T. Thornton, Appl. Phys. Lett. **66**, 3155 (1995).

[3] A. Ourmazd and J. C. Bean, Phys. Rev. Lett. **55**, 765 (1985); V. P. Kesan, F. K. LeGoues, and S. S. Iyer, Phys. Rev. B **46**, 1576 (1992).

[4] For a very complete review of theory and experiment, see A. Zunger and S. Mahajan, in *Handbook on Semiconductors*, edited by T. S. Moss and S. Mahajan (Elsevier Science B.V., Amsterdam, 1994), Vol. 3, pp. 1399–1514.

[5] Wone Keun Han and Jikeun Seo (unpublished).

[6] J. Villain, J. Phys. (France) I **1**, 19 (1991).

[7] P. I. Cohen, G. S. Petrich, P. R. Pukite, G. J. Whaley, and A. S. Arrot, Surf. Sci. **216**, 222 (1989).

[8] A. A. Chernov, *Modern Crystallography III* (Springer-Verlag, Berlin, 1984).

[9] D. J. Eaglesham and M. Cerullo, Phys. Rev. Lett. **64**, 1943 (1990).

[10] J. E. Van Nostrand, S. J. Chey, M.-A. Hasan, D. G. Cahill, and J. E. Greene, Phys. Rev. Lett. **74**, 1127 (1995).

[11] Y. Saito and H. Müller-Krumbhaar, J. Chem. Phys. **74**, 721 (1981).

[12] R. Venkatasubramanian, J. Mater. Res. **7**, 1235 (1992); R. Trivedi, R. Venkatasubramanian, and D. L. Dorsey, in *Common Themes and Mechanisms of Epitaxial Growth*, edited by P. Fuoss, J. Tsao, D. W. Kisker, A. Zangwill, and T. Kuech (MRS, Pittsburgh, 1993), pp. 71–76.

[13] M. Ishimaru, S. Matsumura, N. Kuwano, and K. Oki, Phys. Rev. B **51**, 9707 (1995).

[14] Y. Saito and H. Müller-Krumbhaar, J. Chem. Phys. **70**, 1078 (1979).

[15] See, e.g., F. Ducastelle, Prog. Theor. Phys. Suppl. **115**, 255 (1994).

[16] Details omitted here for brevity are written out in detail for a monolayer problem in J. R. Smith, Jr., and A. Zangwill, Surf. Sci. **316**, 359 (1994).

[17] P. Šmilauer and D. D. Vvedensky, Phys. Rev. B **48**, 17 603 (1993).

[18] W. C. Gear, *Numerical Initial Value Problems for Ordinary Differential Equations* (Prentice-Hall, Englewood Cliffs, NJ, 1971).

[19] S. R. Kurtz, J. M. Olson, D. J. Freidman, A. E. Kibbler, and S. Asher, J. Electron. Mater. **23**, 431 (1994).